Technische Universität München

Fakultät für Medizin

Nuklearmedizinische Klinik und Poliklinik, Klinikum rechts der Isar

Application of PSMA-ligands in the uro-oncological theranostics framework

Andrei Gafita

Vollständiger Abdruck der von der Fakultät für Medizin der Technischen Universität München zur Erlangung des akademischen Grades eines

Doktors der Medizin (Dr. med.)

genehmigten Dissertation.

Vorsitzender:	Prof. Dr. Jürgen Schlegel
Prüfer der Dissertation:	1. Prof. Dr. Matthias Eiber
	2. Prof. Dr. Margitta Retz

Die Dissertation wurde am 21.08.2019 bei der Technischen Universität München eingereicht und durch die Fakultät für Medizin am 05.11.2019 angenommen.

meiner lieben Mutter gewidmet

Table of content

List of Tables

List of Figures

Preliminary remark

The format of this dissertation is publication-based according to §6 (2) “Regulations for the Award of Doctoral Degrees” of the Technical University of Munich as it meets the following criteria:

(1) The dissertation is based on two publications that have been accepted for publication or published in international peer-reviewed journals;

(2) The doctoral candidate is the first author of both publications;

(3) The publication-based dissertation provides a brief description of the scientific problem, problem-solving solutions, results and conclusions achieved and related literature;

(4) The dissertation contains a brief summary of each publication and the doctoral candidate’s individual contribution;

(5) The use of the two publications for the current dissertation was approved by the publisher.

1. INTRODUCTION

1.1. Prostate cancer

1.1.1. Incidence

With an estimated incidence of 1,111,700 cases and an estimated mortality of 307,000 men per year, prostate cancer is one of the most prevalent malignancies worldwide (Ferlay et al., 2015). The prostate cancer incidence varies between regions across the world with the highest rates being noticed in Australia and New Zealand (86.4 per 100,000), and North America (73.7 per 100,000) (Bray et al., 2018), particularly in the USA where the incidence rate was recently reported to be 118.2 per 100,000 (Cronin et al., 2018). In Western and Northern Europe it is also a very common malignancy among men (Bray et al., 2018). It mainly develops in older man with about 6 out of 10 cases being diagnosed in men aged 65 or older and a median age of 66 years old (American Cancer Society: Key Statistics for Prostate Cancer. 2018). Easy access to prostate-specific antigen (PSA) testing is thought to contribute to such high incidence rates. The intention of screening is to detect early disease that is potentially curable. The European Randomized Study of Screening for Prostate Cancer (ERSPC) trial that randomized more than 160,000 men to receive PSA screening or otherwise found substantial reduction in death due to prostate cancer in the PSA-screened arm at the 16-year follow-up analysis (Hugosson et al., 2019). However, it is well-known that in low-risk prostate cancer the PSA screening can lead to over-diagnosis. These clinically insignificant cancers are very unlikely to cause any harm to the patients (Stephan, Rittenhouse, Hu, Cammann, & Jung, 2014). Furthermore, with a globally increasing life-expectancy the incidence of prostate cancer is also expected

to raise. However, at the diagnosis time many patients have a low risk of cancer-related symptoms, metastases and death, with an over 99% 5-years survival late for localized disease (American Cancer Society: Key Statistics for Prostate Cancer. 2018). Therefore, a challenge in assessing prognosis and the expectations for clinical outcome is to understand the dynamic of the disease that changes over time depending of different intrinsic factors or therapies to which the tumor has been exposed.

1.1.2. Clinical states

A dynamic progression model for clinical states accounting for both the untreated and post-treatment history of prostate cancer beginning from diagnosis time point to death has been proposed in 2000 (Scher & Heller, 2000). Each state of the disease represents a clinically significance and a key decision point that can be easily recognized by both patients and physicians. Figure 1 displays the proposed clinical states that are described in detail below:

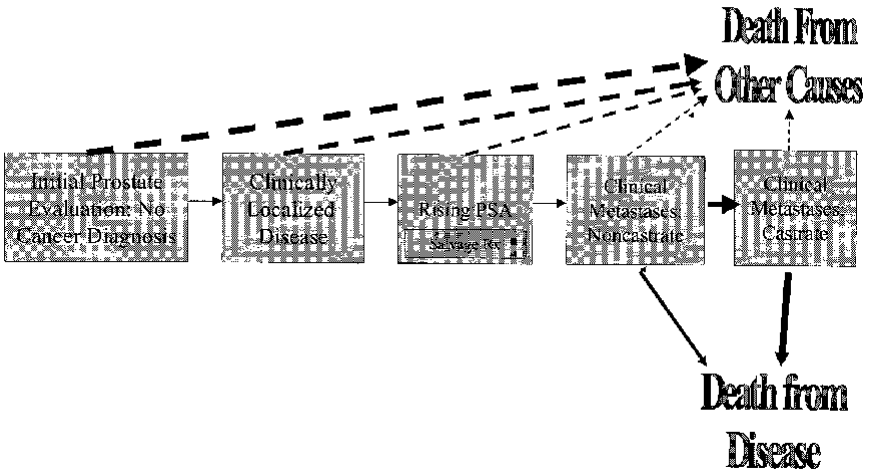

Figure 1. Clinical states model of prostate cancer progression. Dashed line arrows indicate pathways from a clinical state to a non-prostate cancer-related mortality; solid line arrows indicate pathways from a clinical state to a prostate cancer-related mortality

Initial Evaluation

This state consists of patients who are referring to physician for a prostate evaluation with no diagnosis of cancer, including men with high-risk of developing the disease (e.g. elevated serum PSA-levels, positive family history). These patients are regularly followed up using the prostate screening tests (i.e. PSA values, digital rectal examination). Until a histopathology confirmation they remain in the current state.

Localized disease

After diagnosis, patients with histologically confirmed prostate cancer are stratified to distinct risk groups according to their digital-rectal examination results, the serum PSA-levels and histological findings following analysis of the biopsy sample (Mohler et al., 2016; Mottet et al., 2017). In patients with intermediate-risk to high-risk prostate cancer, CT or MRI of the lower abdomen accompanied by bone scintigraphy are recommended in guidelines from the European Association of Urology (Mottet et al., 2017) and the National Comprehensive Cancer Network (Mohler et al., 2016). The clinical practice guidelines for localized disease recommend active surveillance, surgery (radical prostatectomy), external-beam radiation therapy (EBRT) and brachytherapy as alternatives that should be proposed (Sanda et al., 2018).

Biochemical recurrence

Despite primary treatment, some patients with localized prostate cancer will show rising PSA values, a condition known as biochemical recurrence. Approximately 20-40% of patients undergoing surgery (Freedland et al., 2005) and 30-50% of patients receiving EBRT will experience biochemical recurrence within 10 years (Kupelian, Mahadevan, Reddy, Reuther, & Klein, 2006). Despite several definitions for BCR have been proposed, PSA>0.2 ng/ml is the most used one (Tourinho-Barbosa et al.,

2018). In case of BCR, the current standard for detecting metastases involves a bone scan and an abdominopelvic CT scan. Treatment such as salvage radiotherapy or salvage androgen deprivation therapy are currently used in the clinical routine in patients with BCR (Artibani, Porcaro, De Marco, Cerruto, & Siracusano, 2018).

Metastatic disease

Regardless whether the patients are diagnosed with metastatic disease via imaging or by rising PSA values, the cancer has progressed to the point at which the most probable cause of death is cancer and not comorbid conditions. In this disease state, the therapeutic objectives may vary depending on the extent of disease and clinical symptoms. Androgen deprivation therapy (ADT) is the standard treatment, and ADT is typically achieved by medical castration through the use of luteinizing hormone-releasing hormone (LH-RH) agonists (i.e., leuprolide acetate) or LH-RH antagonists (i.e., degarelix acetate). Despite its initial effectiveness in stabilizing or causing regression of metastatic prostate cancer, progression to the lethal form of the disease, known as castration-resistant prostate cancer.

Metastatic castration resistant prostate cancer

Despite its initial effectiveness in stabilizing or causing regression of metastatic prostate cancer, progression to the lethal form of the disease, known as metastatic castration-resistant prostate cancer (mCRPC), is essentially inevitable for these patients. CRPC can be defined as either progressively rising levels of serum tumor marker prostate-specific antigen (PSA) or detection of new or progressive metastatic tumors by radiographic scans, despite castrate testosterone levels (≤50 ng/dL).

While in loco-regional stage the relative 5-year survival rate is 99%, in patients with metastatic prostate cancer it dramatically decreases to 29% (Cronin et al. 2018). Therefore, developing agents that improve survival in mCRPC has become of high interest. Docetaxel was the first cytotoxic agent to show a survival benefit, as well as an improved quality of life, in mCRPC patients (Berthold et al., 2008; Tannock

et al., 2004). In the pivotal TAX 327 phase III trial in 1006 patients with mCRPC, the 3-year survival rate was 18.6% for docetaxel (75 mg/m^2 every 3 weeks) plus prednisone (95% CI 4.9–10.1) (Oudard et al., 2005). Considering these results, a 3-weekly docetaxel regimen became the standard of care for symptomatic patients with mCRPC and asymptomatic patients with progressive disease (Cookson et al., 2013; Heidenreich et al., 2014). In the past years, a variety of new therapeutic agents have been shown to increase overall survival in patients with mCRPC. They include the cytotoxic agent cabazitaxel, the hormone-blocking agents, enzalutamide and abiraterone acetate, bone-targeting radionuclide therapy (Radium-223), and sipuleucel-T immunotherapy (de Bono et al., 2010; Fizazi et al., 2012; Kantoff et al., 2010; Parker et al., 2013; Scher et al., 2012). Despite all these new agents that have been approved, the mCRPC patients have a poor prognosis with an estimated survival of approximately 14 months (Kirby, Hirst, & Crawford, 2011), with more than 250.000 men still die of prostate cancer worldwide each year (Center et al., 2012). Therefore, development of new therapeutic agents for metastatic prostate cancer represents an urgent medical need.

1.2. Prostate-specific membrane antigen as a theranostic target

Prostate-specific membrane antigen (PSMA), also known as glutamate carboxpeptidase II (GCPII) or N-acetyl-L-aspartyl-L-glutamate peptidase I (NAALADase I) is a type II transmembrane glycoprotein that in humans is encoded by the FOLH1 (folate hydrolase 1) (O'Keefe et al., 1998). It is mainly expressed in four tissues of the body, including prostate epithelium, proximal tubules of the kidney, jejunal brush border of the small intestine and ganglia of the nervous system (Barinka et al., 2004; Mhawech-Fauceglia et al., 2007). PSMA expression and localization in the normal human prostate are associated with the cytoplasm and apical side of the epithelium surrounding the prostatic ducts (DeMarzo, Nelson, Isaacs, &

Epstein, 2003). PSMA is enzymatically active only in its dimeric form, but its function for prostate cells is still unknown (Ghosh & Heston, 2004). Dysplastic and neoplastic transformation of prostate tissue results in the transfer of PSMA from the apical membrane to the luminal surface of the ducts (Wright et al., 1996). It has already been shown that PSMA is significantly overexpressed (100-1,000 fold) on prostate cancer cells as compared to normal prostate cells (Mhawech-Fauceglia et al., 2007), its expression being further increased in advanced disease stages, especially in mCRPC. Furthermore, PSMA has a catalytic site in its extracellular domain, which results in its internalization after ligand binding. Beyond PCa, a strong PSMA expression was also seen in the newly formed vessels from other types of carcinomas resembling tumor related angiogenesis (Chang et al., 1999). Noteworthy, the upregulation of PSMA in advanced prostate carcinoma and metastatic disease is also reflected in elevated blood serum levels (Xiao et al., 2001). Due to its above-mentioned characteristics, PSMA has become an attractive target for both diagnostic and treatment of PC (Eiber et al., 2017).

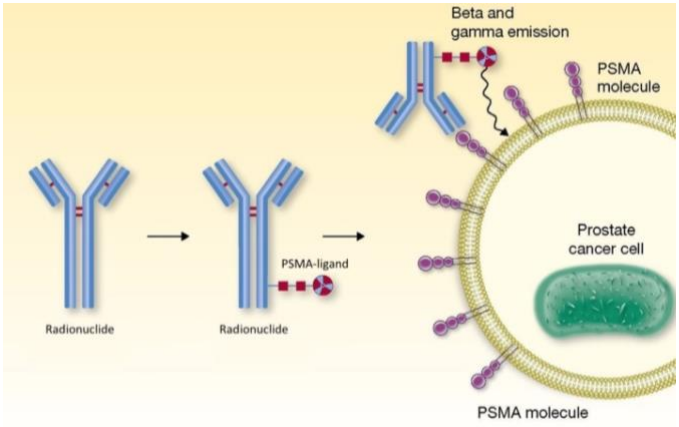

Adapted after *"What's in a Label? Radioimmunotherapy for metastatic prostate cancer"*
Simone et al. Clin Cancer Res 2013

Figure 2. Schematic view of binding radionuclides with PSMA-ligands for targeting PSMA

Several selective PSMA-ligands for radioligand therapy (RLT) have been developed in the past years (Lutje et al., 2015), such as ^{131}I-MIP-1095 (MIP-1095 labelled with ^{131}I) (Zechmann et al., 2014), ^{177}Lu-

PSMA-617 (PSMA-617 labelled with ^{177}Lu) (Ahmadzadehfar et al., 2015), ^{177}Lu-PSMA-I&T (PSMA-I&T labelled with ^{177}Lu) (Heck et al., 2018) or ^{225}Ac-PSMA-617 (PSMA-617 labelled with ^{225}Ac) (Sathekge et al., 2019). While ^{177}Lu is a low-energy beta emitter with an average range within tissue of 0.23 mm and a half-time of 6.64 days, ^{225}Ac is a high-energy alpha emitter with a range within tissue of only 50-100 μm and half-life time of 11.4 days.

^{177}Lu-PSMA RLT has shown encouraging efficacy and a good safety profile. In a retrospective study including 100 patients that received ^{177}Lu-PSMA-I&T (median of 7.4 GBq) up to six cycles, a serum PSA-decline >50% was achieved in 38% of patients, with a median overall survival of 12.9 months. Treatment-emergent hematologic grade 3/4 toxicities were anemia (9%), thrombocytopenia (4%), and neutropenia (6%) and grade 3/4 nonhematologic toxicities were not observed (Heck et al., 2018). In a german multicenter retrospective analysis including 145 patients who received ^{177}Lu-PSMA-617 (range: 2-8 GBq) up to 4 cycles, a 50% PSA-decline was achieved in 45% of patients. Grade 3/4 hematologic toxicities were anemia (10%), thrombocytopenia (4%) and leucopenia (3%). Furthermore, the previous presented results have been confirmed in a prospective setting, in studies involving 30 patients (Hofman, Violet, et al., 2018) and 18 patients (Emmett et al., 2019), with a 50% PSA-decline being observed in 57% and 36% of patients, respectively.

Seventeen patients with mCRPC were treated with 225Ac-PSMA-617 in 2 months interval, with an initial activity of 8 MBq and further de-escalation to 7 MBq, 6 MBq or 4 MBq in case of good therapeutic response. A 90% PSA-decline was noticed in 14 out of 17 (82%) patients, including 7 (41%) patients with undetectable PSA levels who remained in remission 12 months after therapy. Xerostomia grade 1 or 2 was noticed in all patients. One patient showed grade 3 anemia while another patient with solitary kidney and pre-treatment grade 3 renal failure developed grade 4 renal toxicity during RLT (Sathekge et al., 2019).

1.3. Principle of retreatment using the same therapeutic agent: Rechallenge treatment

Exposing a patient to the same oncological treatment, which was effective during primary application is an increasingly used concept in clinical oncology. Different hypotheses supporting this concept have been evoked:

1) Epigenetic changes might drive resistance and treatment could induce these changes. Re-expression of silenced tumor suppressive genes might resensitize tumors to the therapeutic drug. It is therefore possible that a drug holiday (treatment-free interval) could make possible reversion to a previous epigenetic profile. Furthermore, an intermittent treatment could delay acquired resistance.

2) It is plausible that tumor grows as a polyclonal mass. If after an initial response the tumor cell becomes resistant, the retreatment might be successful if changing therapies allows to that clone of cells to re-emerge.

According to a traditional dogma in medical oncology, a patient is defined as being resistant to a certain treatment if the disease fails to respond (called primary resistance) or initially responds with a subsequent progress (secondary resistance) to a specific drug or regimen. Rechallenge therapy is defined as reintroduction of the same therapy to which tumor has already proved to be sensitive and subsequent resistant (Tonini, Imperatori, Vincenzi, Frezza, & Santini, 2013).

This concept has been successfully applied in patients with late-stage prostate cancer. Rechallenge of docetaxel in patients with mCRPC who initially responded to docetaxel chemotherapy regimen was described as a potential treatment option after docetaxel-free interval. Several retrospective studies had reported PSA response rates ranging from 25% to 77% on docetaxel rechallenge after an initial good response to first-line therapy with the drug (Eymard et al., 2010; Loriot et al., 2010; Oudard et al.,

2015). The same concept was also investigated in colorectal cancer using two antibodies targeting the epidermal growth factor receptor, cetuximab and panitumumab (Liu et al., 2015). So far, data for rechallenge of ^{177}Lu-PSMA RLT in patients after prior effective treatment followed by progressive disease after ^{177}Lu-PSMA-free interval has not been investigated. Therefore, we aimed to retrospectively assess the efficacy and safety profile of ^{177}Lu-PSMA rechallenge in this specific patient cohort.

1.4. PSMA-ligand PET quantification

Positron emission tomography (PET) is a three-dimensional imaging technique in nuclear medicine that measure physiological function at a molecular level. PET was introduced in the 1970s by Phelps and Hoffman (Phelps, Hoffman, Mullani, & Ter-Pogossian, 1975). Several PET applications gradually evolved to its first clinical use in neuropsychiatry, cardiology and then in oncology. The most common use of PSMA PET is in oncology with its main use being listed below:

- Primary tumor detection, tumor staging and prognostic stratification

Figure 3. 68-year-old patient presenting with rising PSA-levels up to 12 ng/ml. The axial PET image **(A)** and fused ^{68}Ga-PSMA PET/CT images **(C)** show a focal PSMA-uptake in the left prostate with slightly contrast-enhanced lesion in the CT image **(B)**. Further histopathological evaluation confirmed the primary prostate cancer (Gleason 8).

- Tumor restaging and detection of cancer recurrence

Figure 4. 71-year-old patient with biochemical recurrence (PSA 0.9 ng/ml) after radical prostatectomy. The axial PET **(A)** and fused ^{68}Ga-PSMA PET/CT **(C)** show a high PSMA-uptake in a left iliacal lymph node corresponding to a morphologically unobtrusive lymph node in CT images **(B)**. The histopathology obtained after salvage therapy confirmed a pelvic lymph node metastasis.

- Treatment response assessment

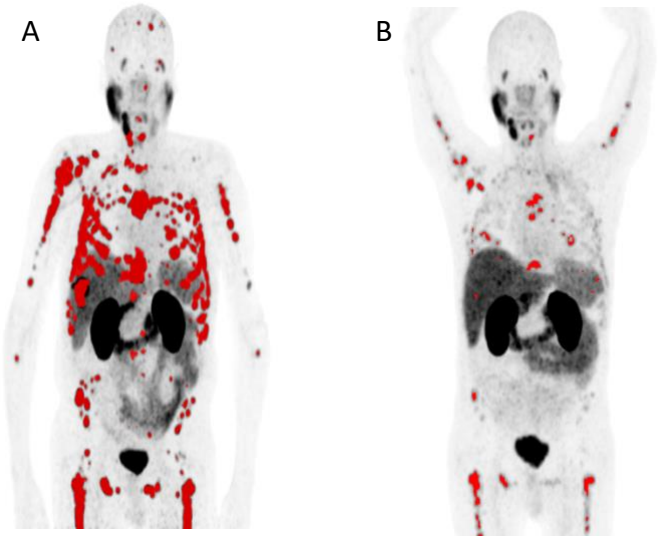

Figure 5. 72-year-old patient with mCRPC with a PSA-value of 472 ng/ml presented for ^{177}Lu-PSMA radioligand therapy. Maximum intensity projection (MIP) of ^{68}Ga-PSMA PET prior to therapy **(A)** shows disseminated skeleton involvement (tumor segmented in red colour). After 3 cycles of ^{177}Lu-PSMA RLT the follow-up ^{68}Ga-PSMA PET MIP **(B)** shows a dramatically therapeutic response also confirmed biochemically with a PSA decline to 35 ng/ml

- Radiotherapy planning

Figure 6. ^{68}Ga-PSMA PET/CT identified solitary L5 metastasis in patient with recurrent prostate cancer after prostatectomy and PSA level of 1. SBRT was used to deliver 18 Gy in single fraction to solitary metastasis. Dose-color-wash shows that 100% of prescribed dose covered target volume while sparing cauda equine (yellow contours).

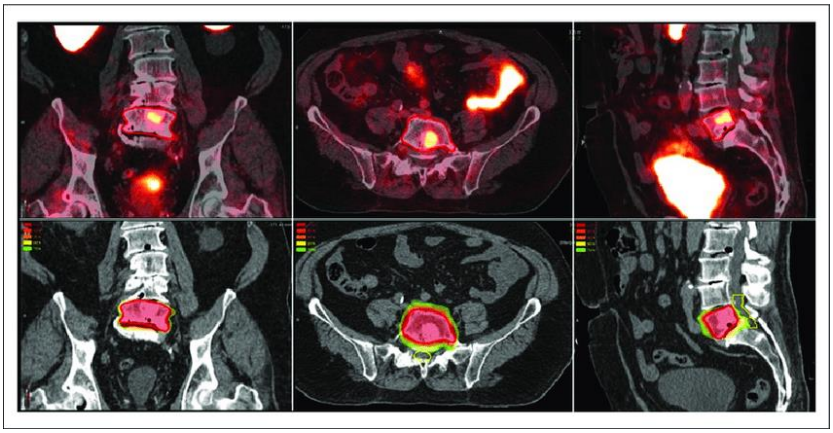

Reference: Calais J, Cao M, Nickols NG. The Utility of PET/CT in External Radiation therapy planning of prostate cancer. J Nucl Med. 2018 Apr; 59(4):557-567

A subsequent important innovation in PET scanners is the combination of PET with computer tomography (CT) resulting the hybrid scanner PET/CT, which allows the combination of anatomical and functional imaging within the same scan procedure. The whole-body CT image is used not only for diagnostic purposes but also in attenuation correction (Kinahan, Townsend, Beyer, & Sashin, 1998). Moving one step forward, the discovery of the Warburg effect (Warburg, Wind, & Negelein, 1927) followed by the development of the fluorinated glucose analogue ^{18}F-fluorodeoxyglucose (^{18}F-FDG) laid the foundation of clinical ^{18}F-FDG PET/CT. In 2007 has been already demonstrated that FDG PET/CT is superior to conventional imaging and PET or CT alone for staging or restaging most malignancies (Czernin, Allen-Auerbach, & Schelbert, 2007). Based on that, PET has become an important imaging technique for precision medicine in clinical oncology. Despite of several new tracers that have been developed in the past years, ^{18}F-FDG still remains the most commonly used radiopharmaceutical for tumor characterization, staging and therapeutic response assessment. Moreover, FDG PET/CT has become a routine investigation in different malignancies, such as lung, lymphoma, esophageal, melanoma, colorectal or breast cancers having a real clinical impact, affecting management decisions regarding different treatment pathway

(Eubank & Mankoff, 2004; Macapinlac, 2004; Vansteenkiste, 2003). Additionally, FDG PET/CT is increasingly adopted in clinical trials as an imaging biomarker, for instance to determine an early therapeutic response to novel drugs or to semi-quantitatively assess the radiographic response (Aridgides, Bogart, Shapiro, & Gajra, 2011). Furthermore, baseline FDG PET-derived tumor burden parameters showed a high predictive value in different malignancies (Mattoli et al., 2017; Mikhaeel et al., 2016).

As mentioned above, new tracers have been developed in the past years. One of the most promising radiopharmaceutical that is increasingly used is compound by labelling gamma-emitters such as ^{68}Ga or ^{18}F with PSMA-ligands. Its high specificity in staging, restaging or therapeutic response assessment proposed it as a promising imaging technique in prostate cancer patients. Several retrospective and recently even prospective analyses have demonstrated the high accuracy of PSMA PET imaging in primary staging, biochemical recurrence in patients with PC (Eiber et al., 2015; Fendler et al., 2019). Several prospective studies have recently shown the superiority of ^{68}Ga-PSMA PET imaging in lesion detection compared to conventional imaging modalities such as bone scan, CT or MRI (Emmett et al., 2018; McCarthy, Francis, Tang, Watts, & Campbell, 2019; Sawicki et al., 2019). In a study of our group, we demonstrated that ^{68}Ga-PSMA11 PET/MRI perform at least equally to clinical nomograms in staging high-risk prostate cancer patients prior to radical prostatectomy (Thalgott et al., 2018).

Furthermore, moving back forward to the theranostic concept in prostate cancer, PSMA PET imaging plays an important role in selecting eligible patients for PSMA-targeted radioligand therapy. Patients who have PSMA-positive lesions expressing SUV-uptake higher than liver can be considered for RLT. Moreover, keeping in mind that “we treat what we see” PSMA PET imaging should at least theoretically be considered the ideal imaging technique for radiographic treatment response assessment during PSMA-targeted RLT. However, studies evaluating its role in assessing therapeutic response during therapy for predictive patients outcome are warranted.

Prostate Cancer Working Group 3 (Scher et al., 2016) does not recommends PSMA-targeted imaging for therapy response assessment and further maintain RECIST 1.1 (Schwartz et al., 2016) for extraskeletal disease evaluation and qualitative interpretation of bone scan as the standard for bone lesions assessment.

Development of a quantitative image-derived biomarker exploiting recent advances in PET-imaging to assess tumor burden based on tumor activity is an unmet clinical need in PC. It is expected to be crucial for accurate evaluation of therapy response. The high accuracy for lesion detection propose PSMA PET imaging as a promising technique to allow tumor load quantification as a candidate image-based biomarker in PC. Still, in patients with high tumor load, manual quantification is time-consuming and a semi-automatic tool would considerably reduce the segmentation time. A first step towards a semi-automatic tumor burden assessment in PC was described in Bieth et al. (Bieth, Kronke, et al., 2017), who proposed a tool that quantifies involvement of skeleton in prostate cancer inspired by the bone scan index (BSI) using ^{68}Ga-PSMA11 PET/CT.

1.5. Project aim

1.5.1 Rechallenge treatment of ^{177}Lu-PSMA

So far, data for rechallenge of ^{177}Lu-PSMA RLT in patients with initial excellent response followed by progressive disease after treatment-free interval has not been published. Therefore, we aimed to retrospectively assess the efficacy and safety profile of ^{177}Lu-PSMA rechallenge.

1.5.2. qPSMA software for PSMA-ligand PET quantification

No previous software for whole-body tumor burden assessment in prostate cancer using PSMA PET imaging has been described in the literature. Therefore, we aimed to describe and validate qPSMA as a tool that allows whole-body semi-automatic tumor burden assessment, i.e. skeletal, lymph node and visceral metastases using ^{68}Ga-PSMA11 PET/CT.

2. MATERIAL AND METHODS

2.1. Rechallenge treatment of ^{177}Lu-PSMA

All patients who received ^{177}Lu-PSMA RLT at our institution between October 2014 and February 2018 were extracted from database. In a second step, patients who successfully completed the initial treatment and subsequently underwent ^{177}Lu-PSMA in a rechallenge setting were included in this analysis. Criteria to consider initial treatment accomplished and to initiate the rechallenge RLT are given in Table 1. All patients received 7.4 GBq during the entire course of treatment. Both initial and rechallenge treatments were performed using a standardized 6-8 week interval between each cycle including a ^{68}Ga-PSMA11 PET/CT every two cycles for radiographic treatment response assessment. All patients signed a written informed consent and were treated under a compassionate use. The institutional review board approved the analysis (reference 115/18S). Patients were treated under a compassionate use protocol (13.2b) which was approved by the local medical ethics committee.

Criteria to consider initial ^{177}Lu-PSMA RLT accomplished:
1. Completion of 4 or 6 cycles
2. At least 50% PSA-decline
3. At least 50% decrease of extent and uptake of metastases on ^{68}Ga-PSMA11 PET
4. Resolution of clinical symptoms if present
Inclusion criteria for rechallenge treatment:
1. Completion of initial ^{177}Lu-PSMA RLT
2. Tumor progression (increasing PSA levels) during ^{177}Lu-PSMA-free interval
3. PSMA-avid lesions on ^{68}Ga-PSMA-11 PET/CT prior to rechallenge treatment

Table 1. Criteria for considering initial treatment accomplished and for initiation of rechallenge treatment

The median patient age at rechallenge treatment was 72 (range: 62-77) years. The median number of ^{177}Lu-PSMA cycles was 6 (range: 4-6) during initial treatment and two (range: 1-4) during rechallenge treatment. Seven patients received at least 2 cycles and two patients underwent at least 3 cycles during rechallenge treatment. The median time of treatment-free interval was 5.4 (range: 3.8-14.7) months. During this interval, all patients received continuous androgen deprivation therapy. Median PSA-level at beginning of rechallenge treatment was 52 (range: 5-2328) ng/ml. Noteworthy, based on the dosimetry results including data for radiation dose limits for normal organs (Okamoto et al., 2017), the maximum number of cycles was initially limited to 4. The rationale for that was not to exceed the dose limit for kidneys which are the critical organ at risk. Due to the fact we have not noticed any relevant treatment-related kidney function impairment (Heck et al., 2016), we subsequently increased the maximum number to 6 cycles for the initial ^{177}Lu-PSMA treatment.

Non-hematological and hematological adverse events were graded according to Common Terminology Criteria for Adverse Events v5.0. The treatment response was assessed using the biochemical, radiographic and clinical parameters. Biochemical response was determined using PSA-decline ≥30%, ≥50%, and ≥90% during both initial and rechallenge treatment. PSA-values were measured at baseline before initiation of ^{177}Lu-PSMA, regularly during every therapy cycle and in the day of ^{68}Ga-PSMA11 PET/CT scan. PERCIST criteria were adopted to ^{68}Ga-PSMA-11 PET/CT to determine radiographic response as described recently (Eiber et al., 2015). Clinical response was assessed by Eastern Cooperative Oncology Group Performance-Status (ECOG PS) and changes in bone pain from the Brief-Pain-Inventory (BPI). Additionally, overall survival and PSA progression-free survival were calculated according to guidelines of the Prostate Cancer Trials Clinical Working Group 3 (Scher et al., 2016).

Overall survival and PSA progression-free survival rates were determined using the Kaplan-Meier curve method with corresponding 95% confidence intervals (95%CI).

2.2. qPSMA software for PSMA-ligand PET quantification

As mentioned in the Introduction section, the second aim of our work was to develop a software that allows for tumor burden assessment in prostate cancer using PSMA PET imaging. In the following part of the thesis we will introduce and validate qPSMA, an in-house developed tool that we have been developing in the nuclear medicine department.

2.2.1. General description of the software

qPSMA reads images in DICOM format. The PET and CT scan are co-registered automatically using the information contained in DICOM headers. The pipeline was written using mainly Python language but also C++ language. The software is running on Ubuntu and can be installed via a virtual machine (i.e. Virtual Box) on any operating system. After finishing the segmentation process, the entire work including the PET, CT and the labels can be saved together into one MATLAB file (.mat). One important step for the software was the implementation of an image interpolation algorithm using cubic B-spline curves (Pan, 2003). This solved a problematic issue in imaging, and namely the intra- and inter-variability in reconstructing different types of PET/CT datasets. Additionally, due to a lack of standardization in protocol scanning, anatomical segments (i.e. head, arms and legs) are not always entirely contained in the field of view of PET/CT images. Therefore, to make possible the comparison between different patients or between different scans of the same patient, the reader can define a specific volume between certain slices to be included in the final statistics. At the end of computation, the maximum intensity projection (MIP) of PET image including the segmentation labels can be displayed. The software includes the possibility to use different standardized uptake value (SUV)-thresholds for skeleton and soft-tissue lesions. This is based on the observation that bone metastases reveal lower PSMA-expression compared to lymph nodes

metastases (Schmittgen, Teske, Vessella, True, & Zakrajsek, 2003), which was confirmed in ^{68}Ga-PSMA11 PET imaging (Freitag et al., 2016).

2.2.2. Software workflow

Figure 8 displays the proposed six-steps workflow of qPSMA for the whole-body tumor segmentation in prostate cancer.

a) Bone mask

The first step computes the bone mask that incorporates the skeleton, which is firstly segmented on the CT. The segmentation method is based on pixel intensities and different morphological operations, as previously described (Bieth, Kronke, et al., 2017; Bieth, Peter, et al., 2017). When necessary, manual corrections can be subsequently applied. As mentioned above, the CT and PET are co-registered using DICOM headers, which also allows to automatically transpose the bone mask to PET images to determine the skeleton location.

b) Normal uptake mask

The second step computes the normal uptake mask includes the organs that typically exhibit high physiological PSMA uptake, i.e. salivary glands, liver, spleen, kidneys and urinary bladder. An algorithm was trained to automatically compute the normal uptake mask, as described (Bieth, Peter, et al., 2017).

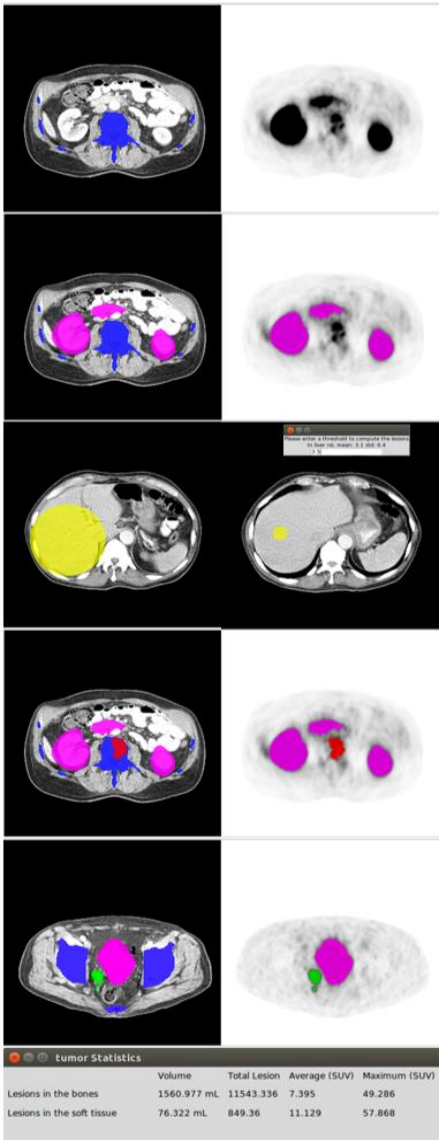

Figure 7. Six-step workflow of qPSMA

c) Liver background activity

The third step computes the average PSMA-uptake within liver. In accordance with PERCIST 1.0 (Wahl, Jacene, Kasamon, & Lodge, 2009) the SUVmean within a 3-cm spherical volume of interest (VOI) within the right liver lobe is used to obtain the liver background activity. In order to minimise the intra- and inter-user variability an algorithm, which showed high reliability and reproducibility in evaluating liver background activity, semi-automatically place the 3-cm VOI (Hirata et al., 2014). Figure 4 display two case examples of patients with liver involvement and placement of 3-VOI in healthy liver tissue using the semi-automatic algorithm.

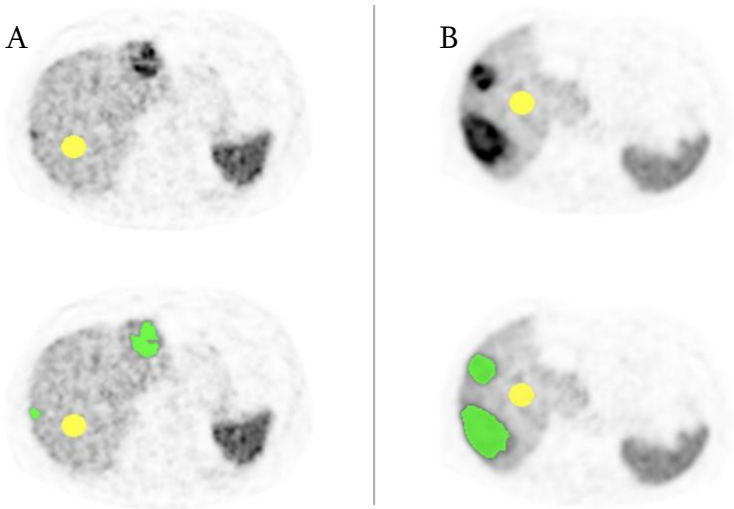

Figure 8. Example of SUVthr_st computation in two prostate cancer patients with liver metastases. Yellow discs represent the automatically computed 3-cm spherical VOI within right liver lobe. The SUVthr_st values were 5.2 (A) and 5.0 (B). Liver metastases were subsequently segmented (green labels).

d) Bone lesions segmentation

The fourth step allows to automatically segment bone lesions. It is well-known that ^{68}Ga-PSMA11 does not usually lead to relevant unspecific uptake within the skeleton. A previous work of our group has previously described a SUVthr_bone of 3 as useful for bone lesion segmentation to omit low background uptake (Bieth, Kronke, et al., 2017). This threshold is applied restricted to voxels within the transposed bone mask from CT. We noticed that due to the spillover effect and misalignments that are frequently present between the CT and PET images (e.g. due to breathing), part of bone lesions can be located outside the bone mask and consequently are improperly segmented as soft-tissue lesions. To overcome this issue, we implemented an automated algorithm that includes the uptake outside the bone mask which is in conjunction to a bone lesions to the respective bone lesions. Figure 5 displays such an example including a rib metastasis, which is partially located outside the bone mask, before and after application of the *'Extend bone lesion'* algorithm.

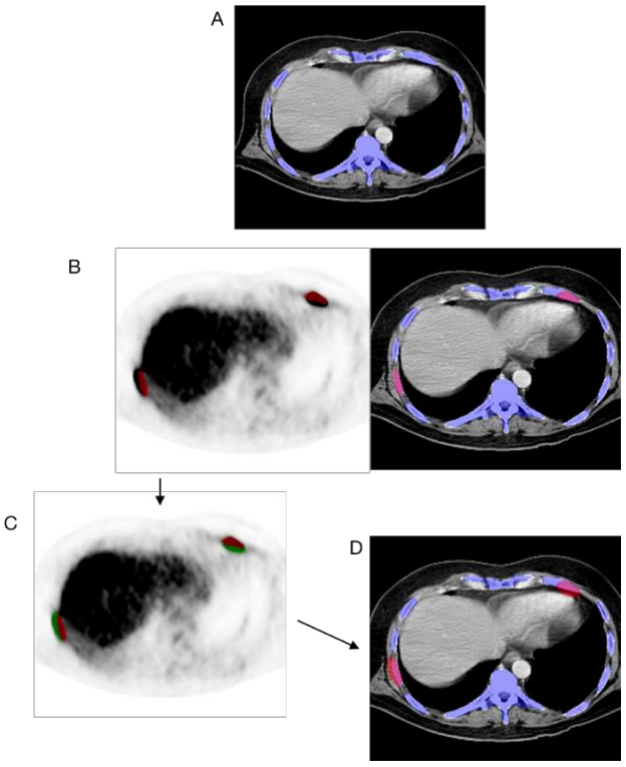

Figure 9. The extend bone lesion algorithm. Firstly, the bone mask is automatically computed **(A)** and the SUV_{thr_bone} is applied **(B)**. Then an SUV_{thr_st} of 3 is computed to segment bone lesions located outside bone mask **(C)**. Finally, the algorithm is applied and soft-tissue lesions that are in conjunction with bone lesions are automatically assigned to bone lesions **(D)**.

e) Soft-tissue lesions segmentation

The fifth step allows to automatically segment the soft-tissue lesions. A separate fixed SUV-threshold for soft-tissue (st) lesions (SUVthr_st) can be applied. The software automatically displays the measured liver background activity (SUVmean + Standard deviation) to assist the user in computing the SUVthr_st. The rationale behind choosing a liver-based threshold a) parallels the recommendation of liver uptake as background as established in PROMISE criteria (Eiber et al., 2018) and b) its physiological ^{68}Ga-PSMA11 uptake, with no detectable PSMA-expression by immunohistochemistry (Silver, Pellicer, Fair, Heston, & Cordon-Cardo, 1997).

Furthermore, the proposed approach allows for using a threshold that is patient- and scan-individualised. Tumor sink effect is a well-known phenomenon in clinical oncology that has shown to influence ^{68}Ga-PSMA11-uptake within different organs (Gaertner et al., 2017). To count for this, the following formula is recommended to be used.

$$SUV_{thr_{st}} = \frac{4.30}{SUV_{mean}} \times (SUV_{mean} + SD)$$

In detail, the value 4.30 represent the average liver SUVmean value obtained in 80 consecutive patients. Finally, after determination of SUVthr_st, all voxels that show SUV > SUVthr_st and are located outside of bone and normal uptake masks are automatically segmented as soft-tissue lesions.

f) Manual corrections

The sixth step allows the user to make manual corrections. Usually, they are necessary to delineate the intestine from abdominal PSMA-ligand positive lymph nodes and to remove false-positive uptake within structures with unspecific uptake such as aorta, esophagus, ureter, rectum, etc. Typical pitfalls in PSMA-ligand PET-imaging (e.g. celiac and other ganglia, adrenal glands) should be taken into

account (Hofman, Hicks, Maurer, & Eiber, 2018). Different tools, such as 'brush', 'erase', 'remove in contour', 'remove whole structure' assist the user in manual corrections. Figure 6 displays two examples of manual corrections that are often required.

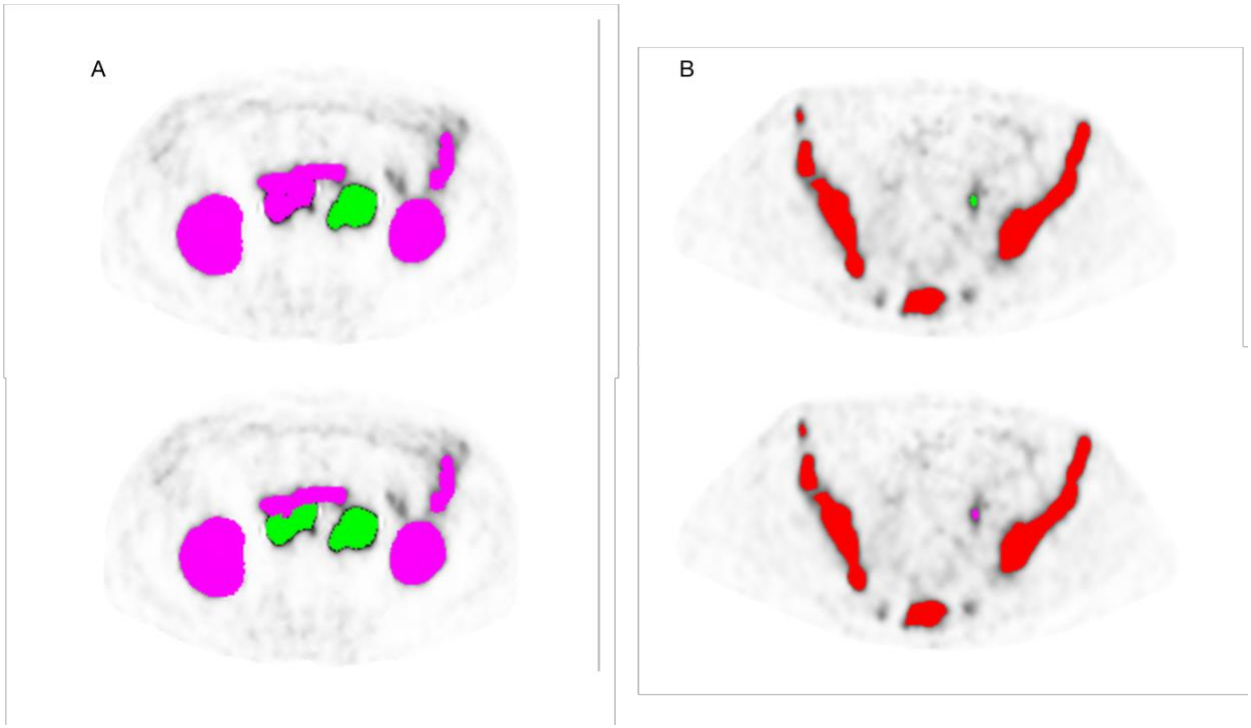

Figure 10. Examples of manual corrections in two mCRPC patients. **(A)** Due to their large connections with the intestine, retroperitoneal lymph nodes were wrongly classified as normal uptake and not taken into account when applied SUVthr_st. After correcting the normal uptake label, the lymph nodes were segmented as soft-tissue lesions. **(B)** Ureter segmented as soft-tissue lesions and manually changed to normal uptake label.

2.2.3. Output parameters

After completing all 6 steps the general statistics can be finally computed. Multiple output parameters are possible and specified in the algorithm. PSMA-Tumor Volume (PSMA-TV), similar to metabolic tumor volume (MTV) from FDG-PET, represents the volume of all PSMA-ligand positive tumor-voxels. PSMA-Total lesion (PSMA-TL), similar to total lesion glycolysis (TLG) from FDG-PET, represents the

total PSMA-activity from all tumor-voxels. PSMA-SUVmean is the average SUV in all PSMA-ligand positive tumor-voxels and PSMA-SUVmax is the voxel with the highest PSMA-expression in the tumor. They are calculated as following, where *N* is the number of *v* tumor-voxels.

$$PSMA\text{-}TV = \sum_{\substack{v\ in \\ lesions}} Voxel_{size}(v)$$

$$PSMA\text{-}SUV_{mean} = \frac{1}{N} \sum_{\substack{v\ in \\ lesions}} SUV(v)$$

$$PSMA\text{-}TL = PSMA\text{-}TV \times PSMA\text{-}SUV_{mean}$$

$$PSMA\text{-}SUV_{max} = Max_{(v\ in\ lesions)}\ SUV(v)$$

All four PET-derived parameters can be calculated separately for soft-tissue lesions (stPSMA-TV, stPSMA-TL, stPSMA-SUVmean, stPSMA-SUVmax) and skeleton lesions (bonePSMA-TV, bonePSMA-TL, bonePSMA-SUVmean, bonePSMA-SUVmax). They are added up to the parameters describing whole-body tumor load (wbPSMA-TV, wbPSMA-TL, wbPSMA- SUVmean, wbPSMA-SUVmax).

2.2.4. Technical validation

The second aim of this analysis was to validate the software, therefore four analyses were performed to validate and evaluate the performance characteristics of qPSMA using 20 ^{68}Ga-PSMA11 PET/CT datasets.

a) Liver threshold validation

The purpose of the first analysis was to evaluate whether the semi-automatic algorithm was proper implemented. The liver-based SUVthr_st was calculated using both qPSMA and the open-source software METAVOL in which it was originally integrated (Hirata et al., 2014).

b) Intra- and inter-observer variability

The objective of this second analysis was to evaluate the reliability using qPSMA. Firstly, we evaluated the inter-variability variability. For that two trained readers used qPSMA and applied manual corrections independently. Secondly, we evaluated the intra-observer reliability and one trained reader analysed the datasets twice at an interval of 4 weeks. For both analyses all computational steps and recommendations were followed as already described. An SUVthr_bone of 3 and a liver-based SUVthr_st were used. To allow for intra-patient comparison, only slices including the trunk between first thoracic vertebrae and lower end of the ischium (both easily recognized on CT) were included.

c) Values validation

With this third analysis, we aimed to validate the obtained values for the outcome parameters. In order to have an accurate validation, we used as a reference a software that is currently used worldwide in the clinical routine for PET imaging. Lesions selected from the 20 ^{68}Ga-PSMA11 PET/CTs were individually segmented using qPSMA and a commercial available software (Syngo.via, Siemens Medical Solutions, Erlangen, Germany).

d) Feasibility

For the last analysis, we aimed to evaluate the practicability and learning curve of using qPSMA, and namely the time spent to analyse the datasets included in the intra-user variability for both reads.

Computational time was counted from the beginning of loading of the bone mask until the output parameters were obtained. Additionally, to assess the feasibility of introducing PSMA-ligand PET-derived tumor burden parameters into a clinical setting, correlations between serum PSA levels and wbPSMA-TV, wbPSMA-TV were evaluated. PSA values were obtained at ±2 weeks of ^{68}Ga-PSMA11 PET/CT acquisition.

2.2.5. Patient cohort for qPSMA software validation

All ^{68}Ga-PSMA11 PET/CT scans were performed at our institution prior to ^{177}Lu-PSMA RLT for patients with advanced prostate cancer. Patients characteristics including age and metastases sites are presented in Table 1. All patients signed a written consent for evaluation of their data. The institutional review board of the Technical University Munich approved this retrospective analysis (permit 5665/13). ^{68}Ga-PSMA11 was administered in compliance with The German Medicinal Products Act, AMG §13(2b), and in accordance with the responsible regulatory body (Government of Oberbayern). ^{68}Ga-PSMA11 was synthesized and PET/CT images were obtained, as described previously (Eiber et al., 2015). The transaxial pixel size was 4.07 mm for PET and 1.52 mm for CT, with a 5 mm slice thickness for both.

No. patients	20
Age, years, mean (range)	73 (65-84)
PSA, ng/ml, mean (range)	369 (1-2222)
Site of metastasis, Pat. No.	
lymph node, overall	12
lymph node only	1
bone, overall	19
bone only	1
bone and lymph node	12
local recurrence	4
visceral, overall	3

Table 2. Patients characteristics

2.2.6. Statistical analysis

Values were reported as mean (range). Relative differences (%) were calculated dividing the absolute value of the differences within the measurements by the average of the two measurements, all multiplied by 100. Means and 95% confidence interval (95%CI) of the relative differences were reported. Paired t-test was used when the values were considered as paired. Intraclass correlation (ICC) estimates and 95%CI were calculated based on a single rater, absolute agreement and 2-way mixed effect model. Spearman's rank correlations were performed to assess the correlations between tumor burden parameters. In each analysis, p value <0.05 was considered statistically significant. All statistical analyses were performed using IBM SPSS Statistics v22.0 (IBM Corp., USA).

3. RESULTS

For the Results section please see attached the two publications:

3.1. ^{177}Lu-PSMA rechallenge treatment

Gafita A, Rauscher I, Retz M, et al. Early experience of rechallenge (177)Lu-PSMA radioligand therapy after an initial good response in patients with mCRPC. *J Nucl Med.* 2018.

3.2. qPSMA software for PSMA-ligand PET quantification

Gafita A, Bieth M, Kroenke M, et al. qPSMA: a semi-automatic software for whole-body tumor burden assessment in prostate cancer using (68)Ga-PSMA11 PET/CT. *J Nucl Med.* 2019.

4. DISCUSSION

4.1. ^{177}Lu-PSMA rechallenge treatment

^{177}Lu-PSMA radioligand therapy is a novel therapeutic option, primarily in patients with mCRPC. It has already shown encouraging results at toxicity level in phase II clinical trial with an estimated progression-free survival of 7 month and overall survival of 13.5 months (Hofman, Violet, et al., 2018). Furthermore, a phase III randomised trial (VISION-trial) has begun to recruit patients with advanced prostate cancer to compare the effect of ^{177}Lu-PSMA RLT with the best supportive care. However, the estimated study completion date is in May 2021 (ClinicalTrials.gov Identifier: NCT03511664).

Currently, in patients who exhibit tumor progress after RLT, with limited further therapeutic options. Most of these patients will have already received all mCRPC treatments such as chemotherapy or novel anti-hormone therapies, such as abiraterone and enzalutamide. Therefore, the retreatment of ^{177}Lu-PSMA could be of interest.

To the best of our knowledge our treatment rechallenge analysis is the first report assessing efficacy and safety profile of ^{177}Lu-PSMA rechallenge in patients with mCRPC. Exposing a patient to the same oncological treatment, which was effective during primary application is an increasingly used concept, e.g. for docetaxel (Heck et al., 2012; Oudard et al., 2015).

In our selected group of patients with excellent response to initial ^{177}Lu-PSMA RLT, the median PSA-PFS during initial therapy course was 12.4 (95%CI: 10.4-14.3) vs. 3.3 (95%CI: 2.6-3.7) months at treatment rechallenge and also shorter compared to an unselected cohort including consecutive patients

that underwent ^{177}Lu-PSMA therapy in a prospective setting (median PSA-PFS 7.6 (95%CI: 6.9-9.0) months (Hofman, Violet, et al., 2018). In the present study, all patients achieved 50% PSA-decline during initial treatment, with only 37.5% of them showing again a 50% PSA-decline during the rechallenge treatment.

In another analysis evaluating patients who were retreated with ^{177}Lu-PSMA, Yordanova et al. reported a median PSA-PFS of 2.8 (range: 1-11) months, with a 50% PSA-decline being noticed in 26, 40 and 20% of patients from the first, second and third rechallenge cycles, respectively (Yordanova et al., 2019). The PSA-PFS was reported only on a cycle-based therefore, the results are difficult to be compared with our analysis. However, in the previously mentioned analysis, a median of 3 (range: 1-5) cycles during initial ^{177}Lu-PSMA while in our cohort a median of 6 (range: 4-6) cycles were performed. This emphasis the fact that our highly selected patients successfully completed the entire course of initial treatment, while in the other study patients showed tumor progress already during first administrations of RLT. Therefore, the results are hardly to be compared.

In a similar setting involving patients who had an initial good response to docetaxel, a 50% PSA-decline was reported in 28-40% of patients at rechallenge treatment (Heck et al., 2012; Oudard et al., 2015). These results outline rechallenge treatment offers antitumor activity, but to a lower extent comparing to initial treatment.

The benefits of any rechallenge treatment should be always weighed against the risk of cumulative toxicity. In our analysis, the three patients who showed grade 3 AEs had already exhibited impaired lab results prior to ^{177}Lu-PSMA rechallenge. Additionally, both patients with grade 3 thrombopenia had substantial tumor progression during rechallenge treatment. Therefore, discriminating bone marrow failure etiology (progression vs. treatment-related) is difficult.

There are currently no guidelines for the maximum number of cycles of ^{177}Lu-PSMA in patients who show good response. Currently, in our institution, the initial treatment with ^{177}Lu-PSMA is typically discontinued after a maximum number of 6 cycles. Noteworthy, therapeutic options that are commonly

used after initial ^{177}Lu-PSMA RLT discontinuation are chemotherapy with Cabazitaxel or radiopharmaceutical Radium-223-dichloride. When compared, the median OS were 14.5 (95%CI: 13.5-15.3), 14.5 (95%CI: 13.5-15.3) and 14.0 (95%CI: 6.2-21.8) months for Cabazitaxel, Radium-223 and our small cohort of ^{177}Lu-PSMA rechallenge, respectively (Eisenberger et al., 2017; Parker et al., 2013). We should be aware that our analysis includes only eight patients, therefore comparison with survival data of other treatments should be done with caution. Based on the limited number of patients, we could not perform advanced analyses, such as predictor factors. However, ^{177}Lu-PSMA RLT has been introduced only recently and therefore the number of patients with an excellent response is limited.

4.2. qPSMA software for PSMA-ligand PET quantification

^{68}Ga-PSMA11 PET/CT is a novel imaging technique in prostate cancer that showed already in prospective studies an enhanced accuracy compared to conventional imaging for lesion detection in patients with recurrent prostate cancer (Fendler et al., 2019). Furthermore, the clinical study "Ga-PSMA-11 in high-risk prostate cancer" from is a phase I/II prospective multicenter analysis that is currently still recruiting patients to compare Ga-PSMA11 PET/CT with conventional in patients with primary disease. Additionally, in the past five years an increased interest has been shown for theranostics concept in prostate cancer, which typically involves a PSMA PET imaging and PSMA-targeted RLT, with ^{177}Lu-PSMA RLT showing encouraging results in a prospective phase II clinical trial (Hofman, Violet, et al., 2018).

Quantification of PSMA PET imaging might of high interest not only in early stage of the disease in evaluating tumor burden to predict the therapeutic response, but also in the framework of theranostics concept for therapy response assessment.

Quantification of FDG PET imaging is increasingly used applying metabolic tumor volume (MTV) and total lesion glycolysis (TLG) as predictor parameters for treatment outcome (Mikhaeel et al., 2016; Rogasch et al., 2018). In PSMA PET imaging, PSMA-avid tumor volume (PSMA-TV) has been introduced as a concordant parameter to MTV and PSMA-Total Lesion (PSMA-TL) to TLG from FDG PET (Schmuck et al., 2017) .

To the best of our knowledge, the introduction of qPSMA as a software for whole-body tumor segmentation is a novel approach towards semi-automatic analysis of PET/CT-data in prostate cancer. Basically, qPSMA integrates various segmentation procedures and PET-quantification into one package to facilitate PSMA-ligand PET tumor burden assessment. In detail, a fixed SUV- threshold is used having liver background activity as a reference for physiological PSMA-ligand uptake, as recommended in PROMISE (Eiber et al., 2018) and computed by using a 3-cm VOI as recommended in PERCIST (Wahl et al., 2009). As novelty, two different thresholds for bone and soft-tissue lesions segmentation were introduced. This takes into consideration their different PSMA-ligand uptake (Freitag et al., 2016; Schmittgen et al., 2003).

Our findings indicate that semi-automatic evaluation of bone, soft-tissue and whole-body tumor load in heavily metastasized prostate cancer patients is feasible, with qPSMA software being a robust software. Values obtained with our in-house developed tool are in high agreement with a commercial software.

A first approach in whole-body tumor burden assessment using ^{68}Ga-PSMA11 PET/CT has been recently introduced in (Schmuck et al. 2017) using an isocontour SUV-threshold method. Due to time consuming process, only patients with low tumor load (<10 lesions) were manually analysed. This resulted in relatively low mean PSMA-TV and PSMA-TL of 3.4mL and 33.2 per patient, respectively. Moreover, a further work (Schmidkonz et al. (Schmidkonz et al., 2018), extended the analysis by evaluating patients with higher tumor burden (PSMA-TV and PSMA-TL of 7.4mL and 73.8, respectively). Despite achievable in patients with low tumor load, such manual segmentation method is time consuming, making whole-body

tumor burden assessment in heavily metastasized patients not feasible. Therefore, a semi-automatic method would pave the way towards a whole-body tumor load quantification in prostate cancer patients. In our analysis, the mean analysed PSMA-TV and PSMA-TL were 823mL and 7273, respectively, indicating that our patient cohort was much more advanced than previous reports in literature using manual segmentation (Schmidkonz et al., 2018; Schmuck et al., 2017). This could also explain the stronger correlations that we obtained between serum PSA and PSMA- ligand PET-derived parameters compared to the previously described (Schmidkonz et al., 2018; Schmuck et al., 2017). Another factor that should be taken into account is that we analysed patients with mCRPC, while these two reports analyzed patients with biochemical recurrence.

Noteworthy, no segmentation method has been yet established for PET as the gold standard. Currently, two methods are largely used for PET quantification, and namely fixed- threshold and isocontour relative-threshold (Mikhaeel et al., 2016; Rogasch et al., 2018; Schmuck et al., 2017). However, it has been shown that despite different results using various segmentation methods or partial volume effect correction, no significant impact on the predictive or prognostic power of PET-derived parameters could be found (Mhawech-Fauceglia et al., 2007; Barinka et al., 2004). This can explain from the statistical point of view by the fact that despite different values for tumor volume are obtained among patients, as long as the statistical order remains the same within the cohort than the prediction value will have same statistical power. Based on the observations, we consequently focused more on the development of a semi-automatic algorithm that makes whole-body tumor burden assessment in heavily metastasized patients feasible than in deeply analyzing differences between segmentation methods. Still, further analyses investigating different segmentations method and their impact on therapy response prediction are warranted.

Regarding the liver, we obtained a SUVmean of 4.30, which is in concordance with data previously reported (4.19) (Gaertner et al., 2017).

Before publishing our data, EBONI (Hammes, Tager, & Drzezga, 2018) was the only software-tool available and published for automatic PSMA-ligand PET image assessment. However, it was introduced as a tool focusing on skeletal tumor load only based on its approach to fully-automatically extract PET-data based on its location within the skeleton on the corresponding CT. A fixed SUV-threshold of 2.5 was found to be the optimal cut-off for bone lesion segmentation. This is in concordance with the SUV-threshold for bone lesions (SUV=3) that was found as the most suitable in one of our previous work (Bieth, Kronke, et al., 2017) and has been further implemented in qPSMA. A drawback of EBONI is the fact that it does not correct for misalignments between the PET and CT and thus will miss parts of bone lesions that are falsely located outside the bone mask due to breathing, movement etc. In qPSMA we implemented an algorithm, which specifically allows automatic recognition of those parts of bone lesion which lie outside the bone mask due to misalignments.

Our in-house developed software also has several limitations that have to be noted. First drawback is the use of liver-based threshold, which limits its use in diffuse liver involvement. Second, lesions with lower PSMA-uptake than liver background activity are missed by the algorithm. Even though currently SUV-based threshold is the state-of-art in PET segmentation, it has been shown that SUV is susceptible to the use of different scanners and reconstruction methods (Adams, Turkington, Wilson, & Wong, 2010). To overcome these issues, for the next version of the software we will focus on shifting from the thresholding to convolutional neural networks, which have already shown enhanced accuracy in PET segmentation, as compared to conventional methods (Hatt et al., 2018).

REFERENCES

Adams, M. C., Turkington, T. G., Wilson, J. M., & Wong, T. Z. (2010). A systematic review of the factors affecting accuracy of SUV measurements. *AJR Am J Roentgenol, 195*(2), 310-320. doi:10.2214/ajr.10.492310.2214/AJR.10.4923.

Ahmadzadehfar, H., Rahbar, K., Kürpig, S., Bögemann, M., Claesener, M., Eppard, E., . . . Essler, M. (2015). Early side effects and first results of radioligand therapy with 177Lu-DKFZ-617 PSMA of castrate-resistant metastatic prostate cancer: a two-centre study *EJNMMI Res* (Vol. 5).

American Cancer Society: Key Statistics for Prostate Cancer. Available at http://www.cancer.org/cancer/prostatecancer/detailedguide/prostate-cancer-key-statistics. (2018).

Aridgides, P., Bogart, J., Shapiro, A., & Gajra, A. (2011). PET Response-Guided Treatment of Hodgkin's Lymphoma: A Review of the Evidence and Active Clinical Trials. *Adv Hematol, 2011*, 309237. doi:10.1155/2011/30923710.1155/2011/309237. Epub 2010 Dec 27.

Artibani, W., Porcaro, A. B., De Marco, V., Cerruto, M. A., & Siracusano, S. (2018). Management of Biochemical Recurrence after Primary Curative Treatment for Prostate Cancer: A Review. *Urol Int, 100*(3), 251-262. doi:10.1159/00048143810.1159/000481438. Epub 2017 Nov 21.

Barinka, C., Sacha, P., Sklenar, J., Man, P., Bezouska, K., Slusher, B. S., & Konvalinka, J. (2004). Identification of the N-glycosylation sites on glutamate carboxypeptidase II necessary for proteolytic activity. *Protein Sci, 13*(6), 1627-1635. doi:10.1110/ps.0462210410.1110/ps.04622104.

Berthold, D. R., Pond, G. R., Soban, F., de Wit, R., Eisenberger, M., & Tannock, I. F. (2008). Docetaxel plus prednisone or mitoxantrone plus prednisone for advanced prostate cancer: updated survival in the TAX 327 study. *J Clin Oncol, 26*(2), 242-245. doi:10.1200/jco.2007.12.400810.1200/JCO.2007.12.4008.

Bieth, M., Kronke, M., Tauber, R., Dahlbender, M., Retz, M., Nekolla, S. G., . . . Schwaiger, M. (2017). Exploring New Multimodal Quantitative Imaging Indices for the Assessment of Osseous Tumor Burden in Prostate Cancer Using (68)Ga-PSMA PET/CT. *J Nucl Med, 58*(10), 1632-1637. doi:10.2967/jnumed.116.189050

Bieth, M., Peter, L., Nekolla, S. G., Eiber, M., Langs, G., Schwaiger, M., & Menze, B. (2018). Segmentation of Skeleton and Organs in Whole-Body CT Images via Iterative Trilateration. *IEEE Trans Med Imaging, 36*(11), 2276-2286. doi:10.1109/tmi.2017.2720261

Bray, F., Ferlay, J., Soerjomataram, I., Siegel, R. L., Torre, L. A., & Jemal, A. (2018). Global cancer statistics 2018: GLOBOCAN estimates of incidence and mortality worldwide for 36 cancers in 185 countries. *CA Cancer J Clin, 68*(6), 394-424. doi:10.3322/caac.21492

Center, M. M., Jemal, A., Lortet-Tieulent, J., Ward, E., Ferlay, J., Brawley, O., & Bray, F. (2012). International variation in prostate cancer incidence and mortality rates. *Eur Urol, 61*(6), 1079-1092. doi:10.1016/j.eururo.2012.02.054

Chang, S. S., O'Keefe, D. S., Bacich, D. J., Reuter, V. E., Heston, W. D., & Gaudin, P. B. (1999). Prostate-specific membrane antigen is produced in tumor-associated neovasculature. *Clin Cancer Res, 5*(10), 2674-2681.

Cookson, M. S., Roth, B. J., Dahm, P., Engstrom, C., Freedland, S. J., Hussain, M., . . . Kibel, A. S. (2013). Castration-resistant prostate cancer: AUA Guideline. *J Urol, 190*(2), 429-438. doi:10.1016/j.juro.2013.05.00510.1016/j.juro.2013.05.005. Epub 2013 May 9.

Cronin, K. A., Lake, A. J., Scott, S., Sherman, R. L., Noone, A. M., Howlader, N., . . . Jemal, A. (2018). Annual Report to the Nation on the Status of Cancer, part I: National cancer statistics. *Cancer, 124*(13), 2785-2800. doi:10.1002/cncr.3155110.1002/cncr.31551. Epub 2018 May 22.

Czernin, J., Allen-Auerbach, M., & Schelbert, H. R. (2007). Improvements in cancer staging with PET/CT: literature-based evidence as of September 2006. *J Nucl Med, 48 Suppl 1*, 78s-88s.

de Bono, J. S., Oudard, S., Ozguroglu, M., Hansen, S., Machiels, J. P., Kocak, I., . . . Sartor, A. O. (2010). Prednisone plus cabazitaxel or mitoxantrone for metastatic castration-resistant prostate cancer progressing after docetaxel treatment: a randomised open-label trial. *Lancet, 376*(9747), 1147-1154. doi:10.1016/s0140-6736(10)61389-x10.1016/S0140-6736(10)61389-X.

DeMarzo, A. M., Nelson, W. G., Isaacs, W. B., & Epstein, J. I. (2003). Pathological and molecular aspects of prostate cancer. *Lancet, 361*(9361), 955-964. doi:10.1016/s0140-6736(03)12779-1

Eiber, M., Fendler, W. P., Rowe, S. P., Calais, J., Hofman, M. S., Maurer, T., . . . Giesel, F. L. (2017). Prostate-Specific Membrane Antigen Ligands for Imaging and Therapy. *J Nucl Med, 58*(Suppl 2), 67s-76s. doi:10.2967/jnumed.116.186767

Eiber, M., Herrmann, K., Calais, J., Hadaschik, B., Giesel, F. L., Hartenbach, M., . . . Fendler, W. P. (2018). Prostate Cancer Molecular Imaging Standardized Evaluation (PROMISE): Proposed miTNM Classification for the Interpretation of PSMA-Ligand PET/CT. *J Nucl Med, 59*(3), 469-478. doi:10.2967/jnumed.117.198119

Eiber, M., Maurer, T., Souvatzoglou, M., Beer, A. J., Ruffani, A., Haller, B., . . . Schwaiger, M. (2015). Evaluation of Hybrid (6)(8)Ga-PSMA Ligand PET/CT in 248 Patients with Biochemical Recurrence After Radical Prostatectomy. *J Nucl Med, 56*(5), 668-674. doi:10.2967/jnumed.115.154153

Eisenberger, M., Hardy-Bessard, A. C., Kim, C. S., Geczi, L., Ford, D., Mourey, L., . . . de Bono, J. (2017). Phase III Study Comparing a Reduced Dose of Cabazitaxel (20 mg/m(2)) and the Currently Approved Dose (25 mg/m(2)) in Postdocetaxel Patients With Metastatic Castration-Resistant Prostate Cancer-PROSELICA. *J Clin Oncol, 35*(28), 3198-3206. doi:10.1200/jco.2016.72.1076

Emmett, L., Crumbaker, M., Ho, B., Willowson, K., Eu, P., Ratnayake, L., . . . Joshua, A. M. (2019). Results of a Prospective Phase 2 Pilot Trial of (177)Lu-PSMA-617 Therapy for Metastatic Castration-Resistant Prostate Cancer Including Imaging Predictors of Treatment Response and Patterns of Progression. *Clin Genitourin Cancer, 17*(1), 15-22. doi:10.1016/j.clgc.2018.09.01410.1016/j.clgc.2018.09.014. Epub 2018 Sep 27.

Emmett, L., Metser, U., Bauman, G., Hicks, R. J., Weickhardt, A., Davis, I. D., . . . Scott, A. (2018). A Prospective, Multi-site, International Comparison of F-18 fluoro-methyl-choline, multi-parametric magnetic resonance and Ga-68 HBED-CC (PSMA-11) in men with High-Risk

Features and Biochemical Failure after Radical Prostatectomy: Clinical Performance and Patient Outcomes. *J Nucl Med*. doi:10.2967/jnumed.118.22010310.2967/jnumed.118.220103.

Eubank, W. B., & Mankoff, D. A. (2004). Current and future uses of positron emission tomography in breast cancer imaging. *Semin Nucl Med, 34*(3), 224-240.

Eymard, J. C., Oudard, S., Gravis, G., Ferrero, J. M., Theodore, C., Joly, F., . . . Beuzeboc, P. (2010). Docetaxel reintroduction in patients with metastatic castration-resistant docetaxel-sensitive prostate cancer: a retrospective multicentre study. *BJU Int, 106*(7), 974-978. doi:10.1111/j.1464-410X.2010.09296.x

Fendler, W. P., Calais, J., Eiber, M., Flavell, R. R., Mishoe, A., Feng, F. Y., . . . Hope, T. A. (2019). Assessment of 68Ga-PSMA-11 PET Accuracy in Localizing Recurrent Prostate Cancer: A Prospective Single-Arm Clinical Trial. *JAMA Oncol*. doi:10.1001/jamaoncol.2019.009610.1001/jamaoncol.2019.0096.

Ferlay, J., Soerjomataram, I., Dikshit, R., Eser, S., Mathers, C., Rebelo, M., . . . Bray, F. (2015). Cancer incidence and mortality worldwide: sources, methods and major patterns in GLOBOCAN 2012. *Int J Cancer, 136*(5), E359-386. doi:10.1002/ijc.2921010.1002/ijc.29210. Epub 2014 Oct 9.

Fizazi, K., Scher, H. I., Molina, A., Logothetis, C. J., Chi, K. N., Jones, R. J., . . . de Bono, J. S. (2012). Abiraterone acetate for treatment of metastatic castration-resistant prostate cancer: final overall survival analysis of the COU-AA-301 randomised, double-blind, placebo-controlled phase 3 study. *Lancet Oncol, 13*(10), 983-992. doi:10.1016/s1470-2045(12)70379-010.1016/S1470-2045(12)70379-0. Epub 2012 Sep 18.

Freedland, S. J., Humphreys, E. B., Mangold, L. A., Eisenberger, M., Dorey, F. J., Walsh, P. C., & Partin, A. W. (2005). Risk of prostate cancer-specific mortality following biochemical recurrence after radical prostatectomy. *Jama, 294*(4), 433-439. doi:10.1001/jama.294.4.43310.1001/jama.294.4.433.

Freitag, M. T., Radtke, J. P., Hadaschik, B. A., Kopp-Schneider, A., Eder, M., Kopka, K., . . . Afshar-Oromieh, A. (2016). Comparison of hybrid (68)Ga-PSMA PET/MRI and (68)Ga-PSMA PET/CT in the evaluation of lymph node and bone metastases of prostate cancer. *Eur J Nucl Med Mol Imaging, 43*(1), 70-83. doi:10.1007/s00259-015-3206-3

Gaertner, F. C., Halabi, K., Ahmadzadehfar, H., Kurpig, S., Eppard, E., Kotsikopoulos, C., . . . Essler, M. (2017). Uptake of PSMA-ligands in normal tissues is dependent on tumor load in patients with prostate cancer. *Oncotarget, 8*(33), 55094-55103. doi:10.18632/oncotarget.19049

Ghosh, A., & Heston, W. D. (2004). Tumor target prostate specific membrane antigen (PSMA) and its regulation in prostate cancer. *J Cell Biochem, 91*(3), 528-539. doi:10.1002/jcb.1066110.1002/jcb.10661.

Hammes, J., Tager, P., & Drzezga, A. (2018). EBONI: A Tool for Automated Quantification of Bone Metastasis Load in PSMA PET/CT. *J Nucl Med, 59*(7), 1070-1075. doi:10.2967/jnumed.117.203265

Hatt, M., Laurent, B., Ouahabi, A., Fayad, H., Tan, S., Li, L., . . . Visvikis, D. (2018). The first MICCAI challenge on PET tumor segmentation. *Med Image Anal, 44*, 177-195. doi:10.1016/j.media.2017.12.00710.1016/j.media.2017.12.007. Epub 2017 Dec 9.

Heck, M. M., Retz, M., D'Alessandria, C., Rauscher, I., Scheidhauer, K., Maurer, T., . . . Eiber, M. (2016). Systemic Radioligand Therapy with (177)Lu Labeled Prostate Specific Membrane Antigen Ligand for Imaging and Therapy in Patients with Metastatic Castration Resistant Prostate Cancer. *J Urol, 196*(2), 382-391. doi:10.1016/j.juro.2016.02.2969

Heck, M. M., Tauber, R., Schwaiger, S., Retz, M., D'Alessandria, C., Maurer, T., . . . Eiber, M. (2018). Treatment Outcome, Toxicity, and Predictive Factors for Radioligand Therapy with (177)Lu-PSMA-I&T in Metastatic Castration-resistant Prostate Cancer. *Eur Urol*. doi:10.1016/j.eururo.2018.11.01610.1016/j.eururo.2018.11.016.

Heck, M. M., Thalgott, M., Retz, M., Wolf, P., Maurer, T., Nawroth, R., . . . Kubler, H. (2012). Rational indication for docetaxel rechallenge in metastatic castration-resistant prostate cancer. *BJU Int, 110*(11 Pt B), E635-640. doi:10.1111/j.1464-410X.2012.11364.x

Heidenreich, A., Bastian, P. J., Bellmunt, J., Bolla, M., Joniau, S., van der Kwast, T., . . . Mottet, N. (2014). EAU guidelines on prostate cancer. Part II: Treatment of advanced, relapsing, and castration-resistant prostate cancer. *Eur Urol, 65*(2), 467-479. doi:10.1016/j.eururo.2013.11.00210.1016/j.eururo.2013.11.002. Epub 2013 Nov 12.

Hirata, K., Kobayashi, K., Wong, K. P., Manabe, O., Surmak, A., Tamaki, N., & Huang, S. C. (2014). A semi-automated technique determining the liver standardized uptake value reference for tumor delineation in FDG PET-CT. *PLoS One, 9*(8), e105682. doi:10.1371/journal.pone.0105682

Hofman, M. S., Hicks, R. J., Maurer, T., & Eiber, M. (2018). Prostate-specific Membrane Antigen PET: Clinical Utility in Prostate Cancer, Normal Patterns, Pearls, and Pitfalls. *Radiographics, 38*(1), 200-217. doi:10.1148/rg.2018170108

Hofman, M. S., Violet, J., Hicks, R. J., Ferdinandus, J., Thang, S. P., Akhurst, T., . . . Sandhu, S. (2018). [(177)Lu]-PSMA-617 radionuclide treatment in patients with metastatic castration-resistant prostate cancer (LuPSMA trial): a single-centre, single-arm, phase 2 study. *Lancet Oncol, 19*(6), 825-833. doi:10.1016/s1470-2045(18)30198-0

Hugosson, J., Roobol, M. J., Mansson, M., Tammela, T. L. J., Zappa, M., Nelen, V., . . . Auvinen, A. (2019). A 16-yr Follow-up of the European Randomized study of Screening for Prostate Cancer. *Eur Urol*. doi:10.1016/j.eururo.2019.02.00910.1016/j.eururo.2019.02.009.

Kantoff, P. W., Higano, C. S., Shore, N. D., Berger, E. R., Small, E. J., Penson, D. F., . . . Schellhammer, P. F. (2010). Sipuleucel-T immunotherapy for castration-resistant prostate cancer. *N Engl J Med, 363*(5), 411-422. doi:10.1056/NEJMoa100129410.1056/NEJMoa1001294.

Kinahan, P. E., Townsend, D. W., Beyer, T., & Sashin, D. (1998). Attenuation correction for a combined 3D PET/CT scanner. *Med Phys, 25*(10), 2046-2053. doi:10.1118/1.59839210.1118/1.598392.

Kirby, M., Hirst, C., & Crawford, E. D. (2011). Characterising the castration-resistant prostate cancer population: a systematic review. *Int J Clin Pract, 65*(11), 1180-1192. doi:10.1111/j.1742-1241.2011.02799.x10.1111/j.1742-1241.2011.02799.x.

Kupelian, P. A., Mahadevan, A., Reddy, C. A., Reuther, A. M., & Klein, E. A. (2006). Use of different definitions of biochemical failure after external beam radiotherapy changes conclusions about relative treatment efficacy for localized prostate cancer. *Urology, 68*(3), 593-598. doi:10.1016/j.urology.2006.03.07510.1016/j.urology.2006.03.075. Epub 2006 Sep 18.

Liu, X., George, G. C., Tsimberidou, A. M., Naing, A., Wheler, J. J., Kopetz, S., . . . Overman, M. J. (2015). Retreatment with anti-EGFR based therapies in metastatic colorectal cancer:

impact of intervening time interval and prior anti-EGFR response. *BMC Cancer, 15*, 713. doi:10.1186/s12885-015-1701-310.1186/s12885-015-1701-3.

Loriot, Y., Massard, C., Gross-Goupil, M., Di Palma, M., Escudier, B., Bossi, A., . . . Fizazi, K. (2010). The interval from the last cycle of docetaxel-based chemotherapy to progression is associated with the efficacy of subsequent docetaxel in patients with prostate cancer. *Eur J Cancer, 46*(10), 1770-1772. doi:10.1016/j.ejca.2010.04.010

Lutje, S., Heskamp, S., Cornelissen, A. S., Poeppel, T. D., van den Broek, S. A., Rosenbaum-Krumme, S., . . . Boerman, O. C. (2015). PSMA Ligands for Radionuclide Imaging and Therapy of Prostate Cancer: Clinical Status. *Theranostics, 5*(12), 1388-1401. doi:10.7150/thno.1334810.7150/thno.13348. eCollection 2015.

Macapinlac, H. A. (2004). FDG PET and PET/CT imaging in lymphoma and melanoma. *Cancer J, 10*(4), 262-270.

Mattoli, M. V., Massaccesi, M., Castelluccia, A., Scolozzi, V., Mantini, G., & Calcagni, M. L. (2017). The predictive value of (18)F-FDG PET-CT for assessing the clinical outcomes in locally advanced NSCLC patients after a new induction treatment: low-dose fractionated radiotherapy with concurrent chemotherapy. *Radiat Oncol, 12*(1), 4. doi:10.1186/s13014-016-0737-010.1186/s13014-016-0737-0.

McCarthy, M., Francis, R., Tang, C., Watts, J., & Campbell, A. (2019). A multicentre prospective clinical trial of (68)Gallium PSMA HBED-CC PET-CT restaging in biochemically relapsed prostate carcinoma: Oligometastatic rate and distribution, compared to standard imaging. *Int J Radiat Oncol Biol Phys*. doi:10.1016/j.ijrobp.2019.03.01410.1016/j.ijrobp.2019.03.014.

Mhawech-Fauceglia, P., Zhang, S., Terracciano, L., Sauter, G., Chadhuri, A., Herrmann, F. R., & Penetrante, R. (2007). Prostate-specific membrane antigen (PSMA) protein expression in normal and neoplastic tissues and its sensitivity and specificity in prostate adenocarcinoma: an immunohistochemical study using mutiple tumour tissue microarray technique. *Histopathology, 50*(4), 472-483. doi:10.1111/j.1365-2559.2007.02635.x10.1111/j.1365-2559.2007.02635.x.

Mikhaeel, N. G., Smith, D., Dunn, J. T., Phillips, M., Moller, H., Fields, P. A., . . . Barrington, S. F. (2016). Combination of baseline metabolic tumour volume and early response on PET/CT improves progression-free survival prediction in DLBCL. *Eur J Nucl Med Mol Imaging, 43*(7), 1209-1219. doi:10.1007/s00259-016-3315-7

Mohler, J. L., Armstrong, A. J., Bahnson, R. R., D'Amico, A. V., Davis, B. J., Eastham, J. A., . . . Freedman-Cass, D. A. (2016). Prostate Cancer, Version 1.2016. *J Natl Compr Canc Netw, 14*(1), 19-30.

Mottet, N., Bellmunt, J., Bolla, M., Briers, E., Cumberbatch, M. G., De Santis, M., . . . Cornford, P. (2017). EAU-ESTRO-SIOG Guidelines on Prostate Cancer. Part 1: Screening, Diagnosis, and Local Treatment with Curative Intent. *Eur Urol, 71*(4), 618-629. doi:10.1016/j.eururo.2016.08.00310.1016/j.eururo.2016.08.003. Epub 2016 Aug 25.

O'Keefe, D. S., Su, S. L., Bacich, D. J., Horiguchi, Y., Luo, Y., Powell, C. T., . . . Heston, W. D. (1998). Mapping, genomic organization and promoter analysis of the human prostate-specific membrane antigen gene. *Biochim Biophys Acta, 1443*(1-2), 113-127.

Okamoto, S., Thieme, A., Allmann, J., D'Alessandria, C., Maurer, T., Retz, M., . . . Eiber, M. (2017). Radiation Dosimetry for (177)Lu-PSMA I&T in Metastatic Castration-Resistant Prostate

Cancer: Absorbed Dose in Normal Organs and Tumor Lesions. *J Nucl Med, 58*(3), 445-450. doi:10.2967/jnumed.116.178483

Oudard, S., Banu, E., Beuzeboc, P., Voog, E., Dourthe, L. M., Hardy-Bessard, A. C., . . . Andrieu, J. M. (2005). Multicenter randomized phase II study of two schedules of docetaxel, estramustine, and prednisone versus mitoxantrone plus prednisone in patients with metastatic hormone-refractory prostate cancer. *J Clin Oncol, 23*(15), 3343-3351. doi:10.1200/jco.2005.12.18710.1200/JCO.2005.12.187. Epub 2005 Feb 28.

Oudard, S., Kramer, G., Caffo, O., Creppy, L., Loriot, Y., Hansen, S., . . . Krainer, M. (2015). Docetaxel rechallenge after an initial good response in patients with metastatic castration-resistant prostate cancer. *BJU Int, 115*(5), 744-752. doi:10.1111/bju.12845

Pan, J. (2003). Image Interpolation using Spline Curves. Retrieved from http://cadcam.eng.sunysb.edu/~purwar/Teaching/MEC572/Term_Papers/Jiahui_Pan_TermPaper.pdf

Parker, C., Nilsson, S., Heinrich, D., Helle, S. I., O'Sullivan, J. M., Fossa, S. D., . . . Sartor, O. (2013). Alpha emitter radium-223 and survival in metastatic prostate cancer. *N Engl J Med, 369*(3), 213-223. doi:10.1056/NEJMoa1213755

Phelps, M. E., Hoffman, E. J., Mullani, N. A., & Ter-Pogossian, M. M. (1975). Application of annihilation coincidence detection to transaxial reconstruction tomography. *J Nucl Med, 16*(3), 210-224.

Rogasch, J. M. M., Hundsdoerfer, P., Hofheinz, F., Wedel, F., Schatka, I., Amthauer, H., & Furth, C. (2018). Pretherapeutic FDG-PET total metabolic tumor volume predicts response to induction therapy in pediatric Hodgkin's lymphoma. *BMC Cancer, 18*(1), 521. doi:10.1186/s12885-018-4432-4

Sanda, M. G., Cadeddu, J. A., Kirkby, E., Chen, R. C., Crispino, T., Fontanarosa, J., . . . Treadwell, J. R. (2018). Clinically Localized Prostate Cancer: AUA/ASTRO/SUO Guideline. Part II: Recommended Approaches and Details of Specific Care Options. *J Urol, 199*(4), 990-997. doi:10.1016/j.juro.2018.01.00210.1016/j.juro.2018.01.002. Epub 2018 Jan 10.

Sathekge, M., Bruchertseifer, F., Knoesen, O., Reyneke, F., Lawal, I., Lengana, T., . . . Morgenstern, A. (2019). 225Ac-PSMA-617 in chemotherapy-naive patients with advanced prostate cancer: a pilot study *Eur J Nucl Med Mol Imaging* (Vol. 46, pp. 129-138).

Sawicki, L. M., Kirchner, J., Buddensieck, C., Antke, C., Ullrich, T., Schimmoller, L., . . . Hautzel, H. (2019). Prospective comparison of whole-body MRI and (68)Ga-PSMA PET/CT for the detection of biochemical recurrence of prostate cancer after radical prostatectomy. *Eur J Nucl Med Mol Imaging*. doi:10.1007/s00259-019-04308-510.1007/s00259-019-04308-5.

Scher, H. I., Fizazi, K., Saad, F., Taplin, M. E., Sternberg, C. N., Miller, K., . . . de Bono, J. S. (2012). Increased survival with enzalutamide in prostate cancer after chemotherapy. *N Engl J Med, 367*(13), 1187-1197. doi:10.1056/NEJMoa120750610.1056/NEJMoa1207506. Epub 2012 Aug 15.

Scher, H. I., & Heller, G. (2000). Clinical states in prostate cancer: toward a dynamic model of disease progression. *Urology, 55*(3), 323-327.

Scher, H. I., Morris, M. J., Stadler, W. M., Higano, C., Basch, E., Fizazi, K., . . . Armstrong, A. J. (2016). Trial Design and Objectives for Castration-Resistant Prostate Cancer: Updated Recommendations From the Prostate Cancer Clinical Trials Working Group 3. *J Clin Oncol, 34*(12), 1402-1418. doi:10.1200/jco.2015.64.2702

Schmidkonz, C., Cordes, M., Schmidt, D., Bauerle, T., Goetz, T. I., Beck, M., . . . Ritt, P. (2018). (68)Ga-PSMA-11 PET/CT-derived metabolic parameters for determination of whole-body tumor burden and treatment response in prostate cancer. *Eur J Nucl Med Mol Imaging*. doi:10.1007/s00259-018-4042-z

Schmittgen, T. D., Teske, S., Vessella, R. L., True, L. D., & Zakrajsek, B. A. (2003). Expression of prostate specific membrane antigen and three alternatively spliced variants of PSMA in prostate cancer patients. *Int J Cancer, 107*(2), 323-329. doi:10.1002/ijc.1140210.1002/ijc.11402.

Schmuck, S., von Klot, C. A., Henkenberens, C., Sohns, J. M., Christiansen, H., Wester, H. J., . . . Derlin, T. (2017). Initial Experience with Volumetric (68)Ga-PSMA I&T PET/CT for Assessment of Whole-Body Tumor Burden as a Quantitative Imaging Biomarker in Patients with Prostate Cancer. *J Nucl Med, 58*(12), 1962-1968. doi:10.2967/jnumed.117.193581

Schwartz, L. H., Litiere, S., de Vries, E., Ford, R., Gwyther, S., Mandrekar, S., . . . Seymour, L. (2016). RECIST 1.1-Update and clarification: From the RECIST committee. *Eur J Cancer, 62*, 132-137. doi:10.1016/j.ejca.2016.03.081

Silver, D. A., Pellicer, I., Fair, W. R., Heston, W. D., & Cordon-Cardo, C. (1997). Prostate-specific membrane antigen expression in normal and malignant human tissues. *Clin Cancer Res, 3*(1), 81-85.

Stephan, C., Rittenhouse, H., Hu, X., Cammann, H., & Jung, K. (2014). Prostate-Specific Antigen (PSA) Screening and New Biomarkers for Prostate Cancer (PCa) *EJIFCC* (Vol. 25, pp. 55-78).

Tannock, I. F., de Wit, R., Berry, W. R., Horti, J., Pluzanska, A., Chi, K. N., . . . Eisenberger, M. A. (2004). Docetaxel plus prednisone or mitoxantrone plus prednisone for advanced prostate cancer. *N Engl J Med, 351*(15), 1502-1512. doi:10.1056/NEJMoa040720 10.1056/NEJMoa040720.

Thalgott, M., Duwel, C., Rauscher, I., Heck, M. M., Haller, B., Gafita, A., . . . Eiber, M. (2018). One-Stop-Shop Whole-Body (68)Ga-PSMA-11 PET/MRI Compared with Clinical Nomograms for Preoperative T and N Staging of High-Risk Prostate Cancer. *J Nucl Med, 59*(12), 1850-1856. doi:10.2967/jnumed.117.20769610.2967/jnumed.117.207696. Epub 2018 May 24.

Tonini, G., Imperatori, M., Vincenzi, B., Frezza, A. M., & Santini, D. (2013). Rechallenge therapy and treatment holiday: different strategies in management of metastatic colorectal cancer. *J Exp Clin Cancer Res, 32*, 92. doi:10.1186/1756-9966-32-9210.1186/1756-9966-32-92.

Tourinho-Barbosa, R., Srougi, V., Nunes-Silva, I., Baghdadi, M., Rembeyo, G., Eiffel, S. S., . . . Sanchez-Salas, R. (2018). Biochemical recurrence after radical prostatectomy: what does it mean? *Int Braz J Urol* (Vol. 44, pp. 14-21).

Vansteenkiste, J. F. (2003). PET scan in the staging of non-small cell lung cancer. *Lung Cancer, 42 Suppl 1*, S27-37.

Wahl, R. L., Jacene, H., Kasamon, Y., & Lodge, M. A. (2009). From RECIST to PERCIST: Evolving Considerations for PET response criteria in solid tumors. *J Nucl Med, 50 Suppl 1*, 122s-150s. doi:10.2967/jnumed.108.057307

Warburg, O., Wind, F., & Negelein, E. (1927). THE METABOLISM OF TUMORS IN THE BODY. *J Gen Physiol, 8*(6), 519-530.

Wright, G. L., Jr., Grob, B. M., Haley, C., Grossman, K., Newhall, K., Petrylak, D., . . . Moriarty, R. (1996). Upregulation of prostate-specific membrane antigen after androgen-deprivation therapy. *Urology, 48*(2), 326-334.

Xiao, Z., Adam, B. L., Cazares, L. H., Clements, M. A., Davis, J. W., Schellhammer, P. F., . . . Wright, G. L., Jr. (2001). Quantitation of serum prostate-specific membrane antigen by a novel protein biochip immunoassay discriminates benign from malignant prostate disease. *Cancer Res, 61*(16), 6029-6033.

Yordanova, A., Linden, P., Hauser, S., Meisenheimer, M., Kurpig, S., Feldmann, G., . . . Ahmadzadehfar, H. (2019). Outcome and safety of rechallenge [(177)Lu]Lu-PSMA-617 in patients with metastatic prostate cancer. *Eur J Nucl Med Mol Imaging, 46*(5), 1073-1080. doi:10.1007/s00259-018-4222-x10.1007/s00259-018-4222-x. Epub 2018 Nov 24.

Zechmann, C. M., Afshar-Oromieh, A., Armor, T., Stubbs, J. B., Mier, W., Hadaschik, B., . . . Haberkorn, U. (2014). Radiation dosimetry and first therapy results with a (124)I/ (131)I-labeled small molecule (MIP-1095) targeting PSMA for prostate cancer therapy. *Eur J Nucl Med Mol Imaging, 41*(7), 1280-1292. doi:10.1007/s00259-014-2713-y10.1007/s00259-014-2713-y. Epub 2014 Feb 28.

Summary of publications

Publication #1: Early experience of Rechallenge 177Lu-PSMA radioligand therapy after an initial good response in patients with advanced prostate cancer

Aim: To retrospectively evaluate the efficacy and safety profile of ^{177}Lu-prostate-specific membrane antigen (^{177}Lu-PSMA) radioligand therapy in a rechallenge setting.

Material and Methods: The rechallenge treatment was defined as the subsequent therapy with 177Lu-PSMA-I&T after an initial exposure during what patients showed an excellente response followed by progression. Biochemical, radiographic and clinical antitumor response and toxicity were assessed. Prostate-specific antigen (PSA) progression-free survival (PFS) and overall survival were measured from treatment initiation.

Results: Eight patients underwent a median of 2 cycles of rechallenge with ^{177}Lu-PSMA-I&T. A maximum PSA decline of 50% was achieved in 3 patients (37.5%). Radiographic response was favorable in 3 patients, whereas 4 exhibited progressive disease. Eastern Cooperative Oncology Group performance status was stable during therapy in all patients. No grade 4 toxicity was noticed, while grade 3 toxicity occurred in 3 patients (37.5%). The median PSA-PFS and overall survival were 3.2 months (95% confidence interval, 2.6-3.7 months) and 14.0 months (95% confidence interval, 6.2-21.8 months), respectively.

Conclusion: In a small patient cohort with an initial excellent response, ^{177}Lu-PSMA rechallenge is still active, with lower efficacy and higher toxicity.

Doctoral candidate's individual contribution:

The doctoral candidate contributed to study's design, data acquisition, data analysis and in writing the manuscript.

Publication #2: qPSMA: a semi-automatic software for whole-body tumor burden assessment in prostate cancer using 68Ga-PSMA11 PET/CT

Aim: To validate qPSMA, a semi-automatic software for whole-body tumor burden assessment in prostate cancer patients using ^{68}Ga-Prostate-specific membrane antigen (PSMA)-11 PET/CT.

Material and Methods: Using qPSMA four output parameters are obtained: PSMA-positive tumor volume (PSMA-TV), PSMA-positive total lesion (PSMA-TL), PSMA-SUVmean and PSMA-SUVmax. We used 20 PSMA-targeted PET/CT scans to validate and evaluate the performance characteristics of qPSMA. Four analyses were performed: (1) validation of the semi-automatic algorithm for liver background activity evaluation, (2) assessment of intra- and interobserver variability, (3) comparison of data obtained using qPSMA and a commercial software, and (4) assessment of computational time and evaluation of the correlations between PSMA PET-derived parameters and serum prostate-specific antigen (PSA).

Results: Automatic liver background calculation showed a high correlation with METAVOL. Intra- and interobserver variability analyses showed high agreement. The comparison between qPSMA and the commercial showed no significant differences between the values obtained with the two software packages. The first and second read resulted in mean computational times of 13.63 and 9.27 minutes, respectively (P = 0.001). High significant correlations were found between PSA-value and both PSMA-TV ($r=0.72$, $p<0.001$) and PSMA-TL ($r=0.66$, P = 0.002).

Conclusion: Semi-automatic analyses of whole-body tumor burden in ^{68}Ga-PSMA11 PET/CT is feasible. qPSMA is a robust software that can assist physicians to quantify tumor load in heavily metastasized prostate cancer patients.

Doctoral candidate's individual contribution:

The doctoral candidate contributed to the software's development, study design, data acquisition, data analysis, and in writing the manuscript.

Acknowledgements

Because the mentors are guiding us through life and the companions are teaching us to stay alive…

For the mentoring - I would like to express my gratitude to my thesis supervisor Prof. Dr. Matthias Eiber for his continuous support and patience. I would like to thank PD. Dr. Matthias Heck and Prof. Dr. Wolfgang Weber for their generous supports. I would like to thank Prof. Dr. Markus Schwaiger for paving the way for this dissertation.

For the companions - I am grateful to my family, especially to my mom, for their love and patience. I wish to thank to my friends for their encouragement and to Lukas Bisorca-Gassendorf for his everlasting support.

Another life's chapter has now been accomplished. Looking forward for the next one…

Appendix